



Research paper

Impacts of climate and tree morphology on tree-ring stable isotopes in central Mongolia

Caroline Leland 1,2,11, Laia Andreu-Hayles 1,3,4, Edward R. Cook 1, Kevin J. Anchukaitis 5, Oyunsanaa Byambasuren 6,7, Nicole Davi 1,2, Amy Hessl 8, Dario Martin-Benito 9, Baatarbileg Nachin 1,7 and Neil Pederson 10

¹Lamont-Doherty Earth Observatory of Columbia University, 61 Route 9W, Palisades, NY 10964 USA; ²Department of Environmental Science, William Paterson University, 300 Pompton Rd., Wayne, NJ 07470 USA; ³CREAF, Bellaterra (Cerdanyola del Valles), Barcelona, Spain; ⁴ICREA Pg. Lluís Companys 23, Barcelona, Spain; ⁵Laboratory of Tree-ring Research and School of Geography, Development, and Environment, University of Arizona, 1064 E. Lowell St., Tucson, AZ 85721 USA; ⁶Fire Management Resource Center - Central Asia Region, National University of Mongolia, Building 3, 14201 Ulaanbaatar, Mongolia; ⁷Department of Environment and Forest Engineering, National University of Mongolia, Building 3, 14201, Ulaanbaatar, Mongolia; ⁸Department of Geology and Geography, West Virginia University, 98 Beechurst Ave., Morgantown, WV 26506, USA; ⁹Institute of Forest Sciences (ICIFOR), INIA-CSIC, Ctra. de La Coruña, km. 7.5, 28040 Madrid, Spain; ¹⁰Harvard Forest, 324 N. Main St, Petersham, MA 01366, USA; ¹¹Corresponding author. (cleland@ldeo.columbia.edu)

Received June 17, 2022; accepted December 11, 2022; handling Editor Lucas Cernusak

Recent climate extremes in Mongolia have ignited a renewed interest in understanding past climate variability over centennial and longer time scales across north-central Asia. Tree-ring width records have been extensively studied in Mongolia as proxies for climate reconstruction, however, the climate and environmental signals of tree-ring stable isotopes from this region need to be further explored. Here, we evaluated a 182-year record of tree-ring δ^{13} C and δ^{18} O from Siberian Pine (*Pinus sibirica* Du Tour) from a xeric site in central Mongolia (Khorgo Lava) to elucidate the environmental factors modulating these parameters. First, we analyzed the climate sensitivity of tree-ring δ^{13} C and δ^{18} O at Khorgo Lava for comparison with ring-width records, which have been instrumental in reconstructing hydroclimate in central Mongolia over two millennia. We also compared stable isotope records of trees with partial cambial dieback ('strip-bark morphology'), a feature of long-lived conifers growing on resource-limited sites, and trees with a full cambium ('whole-bark morphology'), to assess the inferred leaf-level physiological behavior of these trees. We found that interannual variability in tree-ring δ^{13} C and δ^{18} O reflected summer hydroclimatic variability, and captured recent, extreme drought conditions, thereby complementing ring-width records. The tree-ring δ^{18} O records also had a spring temperature signal and thus expanded the window of climate information recorded by these trees. Over longer time scales, strip-bark trees had an increasing trend in ring-widths, δ^{13} C (and intrinsic water-use efficiency, iWUE) and δ^{18} O. relative to whole-bark trees. Our results suggest that increases in iWUE at this site might be related to a combination of leaf-level physiological responses to increasing atmospheric CO₂, recent drought, and stem morphological changes. Our study underscores the potential of stable isotopes for broadening our understanding of past climate in north-central Asia. However, further studies are needed to understand how stem morphological changes might impact stable isotopic trends.

Keywords: central Asia, drought, gas-exchange, stable carbon isotopes, stable oxygen isotopes, strip-bark.

Introduction

Mongolia and surrounding regions of arid north-central Asia have experienced extreme changes in temperature and hydroclimate since the onset of the industrial era. The 20th and 21st centuries were defined by rapidly increasing temperatures in Mongolia (D'Arrigo et al. 2000, Davi et al. 2015, 2021), and one of the most severe droughts during the last two millennia occurred at the turn of the 21st century (Pederson et al. 2013, 2014, Hessl et al. 2018). Severe drought, in combination with harsh winter conditions, have cascading negative impacts on communities within Mongolia, particularly nomadic pastoralists (Rao et al. 2015, Kakinuma et al. 2019), and there are concerns about the human and ecological impacts of future climatic change in this region.

Numerous tree-ring width records across Mongolia have been analyzed to assess the sensitivity of tree growth to climate in this region of Asia, and have been critical for reconstructing past climate over the Common Era. These records are valuable for quantifying the range of climatic variability over several centuries into the past, and for determining how this variability compares with climate change projections (Hessl et al. 2018, Davi et al. 2021). Ring-width has been the most analyzed tree-ring parameter in Mongolia for both temperature and drought-limited sites (e.g., Jacoby et al. 1996, D'Arrigo et al. 2000, Pederson et al. 2013, Davi et al. 2015, Hessl et al. 2018). More recently, blue intensity (BI), a measurement of blue light reflectance as a parameter of relative-density (e.g., McCarroll et al. 2002, Campbell et al. 2007, Björklund et al. 2021), has been found to capture temperature variability in trees from high-elevation sites in Mongolia (Davi et al. 2021). Although the climate signals in treering stable isotopes have been explored in regions surrounding Mongolia, such as North China and the Russian Altai (e.g., Liu et al. 2009, Loader et al. 2010, Sidorova et al. 2013, Liu et al. 2019a, 2019b, Kang et al. 2022), to our knowledge, little tree-ring stable isotope research has been done in Mongolia. Tree-ring stable isotopes hold great promise for understanding tree physiological responses to environmental changes as well as for reconstructing different aspects of climatic variability in

Stable carbon (δ^{13} C) and oxygen (δ^{18} O) isotope ratios in tree-ring cellulose can reflect physiological processes occurring within trees, such as gas-exchange variability at the leaf level (McCarroll and Loader 2004, Gagen et al. 2004). Tree-ring stable isotope records can complement or provide different information than radial growth data on how trees respond to changing environmental conditions. Tree-ring δ^{13} C principally captures the ratio between intercellular and ambient CO_2 concentrations (c_i/c_a), which is influenced by assimilation rate and stomatal conductance. Both assimilation and stomatal conductance are influenced by many factors, including climate, sunlight, atmospheric CO_2 concentration, and tree size or developmental

changes (Farguhar et al. 1989; McCarroll and Loader 2004; Klesse et al. 2018). Tree-ring δ^{13} C is also used to infer changes in the intrinsic water-use efficiency (iWUE), or the ratio of net assimilation to stomatal conductance at leaf level, over time. Changes in iWUE are often assessed in relation to increasing atmospheric CO₂ concentrations (e.g., Saurer et al. 2004, Frank et al. 2015), though the factors underlying iWUE trends are complex (e.g., Brienen et al. 2017, Marchand et al. 2020). The $\delta^{18} {\rm O}$ of tree-ring cellulose is influenced by the $\delta^{18} {\rm O}$ of source water, such as precipitation or ground water, but with modifications due to evaporation from the soil and/or leaflevel evaporative enrichment (McCarroll and Loader 2004, Barbour 2007). Tree-ring stable isotopes are key for inferring the physiological response of trees to environmental change and can provide valuable insights on past climate changes in Mongolia.

Tree-ring stable isotopes can also capture changes in leaf or stem morphological factors that affect hydraulic resistance or demand, such as tree height or leaf area to sapwood area ratio (Klesse et al. 2018 and references therein). In a few treering sites across Mongolia, ancient trees growing under extreme environmental conditions exhibit a characteristic signature of longevity known as partial cambial dieback or strip-bark morphology (Wright and Mooney 1965, LaMarche 1969). Partial cambial dieback occurs when one or multiple vertical axes of the stem die in response to environmental stress or a localized loss of resources, and annual growth layers are added only to the living portion of the stem. The factors causing partial cambial dieback vary, but can include damage from wind-blown ice or dirt particles (Schauer et al. 2001, Boyce and Lubbers 2011), or root mortality from rock fall or severe drought (Larson 2001, Matthes et al. 2002). In central Mongolia, cold and dry conditions, coupled with extreme temperature fluctuations from solar radiation, are hypothesized to contribute to stripbark morphology of Siberian Pine (Leland et al. 2018). Whether partial cambial dieback can have an influence on the leaf-level behavior of trees, which can be inferred from tree-ring stable isotope records, is largely unexplored.

Some studies have reported that strip-bark trees show larger, recent increasing trends in ring-widths relative to whole-bark trees (Graybill and Idso 1993, Bunn et al. 2003, Leland et al. 2018), though standardization methods can complicate interpretation of these comparisons (Salzer et al. 2009). Trend differences related to morphological characteristics could potentially bias tree-ring based climate reconstructions if not considered in data processing (Pederson et al. 2014, Hessl et al. 2018, Leland et al. 2018). It is still not well understood why this phenomenon occurs, and whether it occurs broadly across different species and sites. In Graybill and Idso (1993), radial growth differences of strip-bark Bristlecone Pine (though see Salzer et al. 2009) was hypothesized to reflect a carbon

fertilization signal, where strip-bark trees allocate newly acquired carbon to stem growth, whereas whole-bark trees direct a higher proportion of carbon to root and reproductive growth. Tang et al. (1999) found no significant difference in iWUE between strip-bark and whole-bark Bristlecone Pine over the past two centuries based on tree-ring stable isotopes. However, the potential effect of partial cambial dieback on gasexchange of other species has not been tested. Evaluating stable isotope records from strip-bark trees would provide clues on their leaf-level physiological behavior, and assessing whether or not stable isotope trends are different between stripbark and whole-bark trees would have important implications in using these records for paleoclimatic reconstructions. If tree-ring stable isotopes are not subject to the same trend biases identified in ring-widths of some strip-bark trees, these parameters might provide a viable alternative for reconstructing past climate.

In this study, we explore the climatic and leaf-level physiological information captured by tree-ring stable isotopes from long-lived Siberian Pine (Pinus sibirica Du Tour) growing on a xeric site of the Khangai Mountains in Mongolia (the Khorgo Lava field) from 1830 to 2011 CE. Radial tree growth at this site is acutely sensitive to changes in soil moisture availability and these records have been instrumental in reconstructing hydroclimatic variability in central Mongolia exceeding the last 2000 years (Davi et al. 2006, Pederson et al. 2014, Hessl et al. 2018). A high proportion of trees, especially older individuals, exhibit some degree of strip-bark morphology, and increasing trends in strip-bark ring-width records relative to whole-bark trees at this site have been previously described (Leland et al. 2018). Here, we analyze tree-ring stable isotopes $(\delta^{13}C)$ and $\delta^{18}O)$ over the last two centuries to evaluate the climatic information captured by these records, and to assess long-term stable isotope and iWUE trends of strip-bark and whole-bark trees. This research is vital for inferring the gasexchange behavior of these long-lived trees and for determining the suitability of their stable isotope records for paleoclimate reconstruction.

Methods

Sample collection and preparation

We analyzed stable isotope records from six Siberian Pine trees from an ancient lava field located in the northern Khangai Mountains of central Mongolia (Khorgo Lava; 48.16° N, 99.84° E, elevation: \sim 2060 m a.s.l.; Figure 1a and c, Table 1). This semiarid region of Mongolia is defined by an extremely continental climate and the peak of precipitation and mean temperature occurs during summer months (June–August; Figure 1b). The tree cores that were selected for stable isotopic analysis (see selection criteria below) were collected during three separate

sampling trips (summer of 2012, 2014 and 2015) and ring-width records from these samples were also incorporated in earlier studies (Pederson et al. 2014, Hessl et al. 2018, Leland et al. 2018). Specifically, cores from four of the six trees analyzed in this study (SB2, SB3, WB2 and WB3) were sampled and used for a larger comparison of strip-bark and whole-bark ring-width patterns from Khorgo Lava trees in Leland et al. (2018). The other two samples (SB1 and WB1) were collected during other field campaigns, and their ring-width records were previously used for reconstructions of past hydroclimate at Khorgo Lava (Pederson et al. 2014, Hessl et al. 2018).

During all sampling trips, we recorded whether trees had partial cambial dieback ('strip-bark morphology', SB, e.g., Figure 1d) or a fully living cambium ('whole-bark morphology', WB, e.g., Figure 1e). The samples analyzed here were from trees that grew directly on lava rock or thin soils (Figure 1c), and were open-grown, with little to no competition from surrounding trees. These growing conditions are important to minimize potential trends in stable isotope ratios associated with light competition (Buchmann et al. 1997, Brienen et al. 2017, Klesse et al. 2018). In most cases, SB trees are older than WB trees at Khorgo Lava; this age difference is also reflected in our study, though all trees were older than 300 years old when sampled (Table 1). One core was selected from each of the six selected trees for stable isotope analysis.

The selection process for the six samples was based on three criteria: (i) the cores were solid and had rings large enough to cut and enough material to be analyzed, especially given the small growth rings during the recent 21st century drought; (ii) the trees were at least 100 years old prior to the first ring used for stable isotope measurement (year 1830) in order to avoid any juvenile effect on stable isotope ratios (Francey and Farquhar 1982, Duquesnay et al. 1998, Gagen et al. 2007) and (iii) three of the samples came from SB trees and three came from WB trees. The selected SB trees had varying degrees of cambial dieback, and in all cases, the WB trees had a fully living cambial band and were accompanied with a full, broad crown. Table 1 shows the percentage of dead stem circumference associated with each analyzed SB tree, if that information was provided at the time of sampling. An increase in mean ringwidths of SB trees relative to WB trees at Khorgo Lava was previously reported in Leland et al. (2018), though the degree to which individual SB trees showed a higher trend relative to WB trees varied. Here, SB samples showed a clear signature of increasing radial growth trends relative to the WB samples during the last 200 years.

Tree-ring width records

Tree-ring width measurements from the six cores, which were previously used in earlier studies, were also assessed here to complement analyses of the stable isotope records from the same trees. Increment cores were prepared following standard

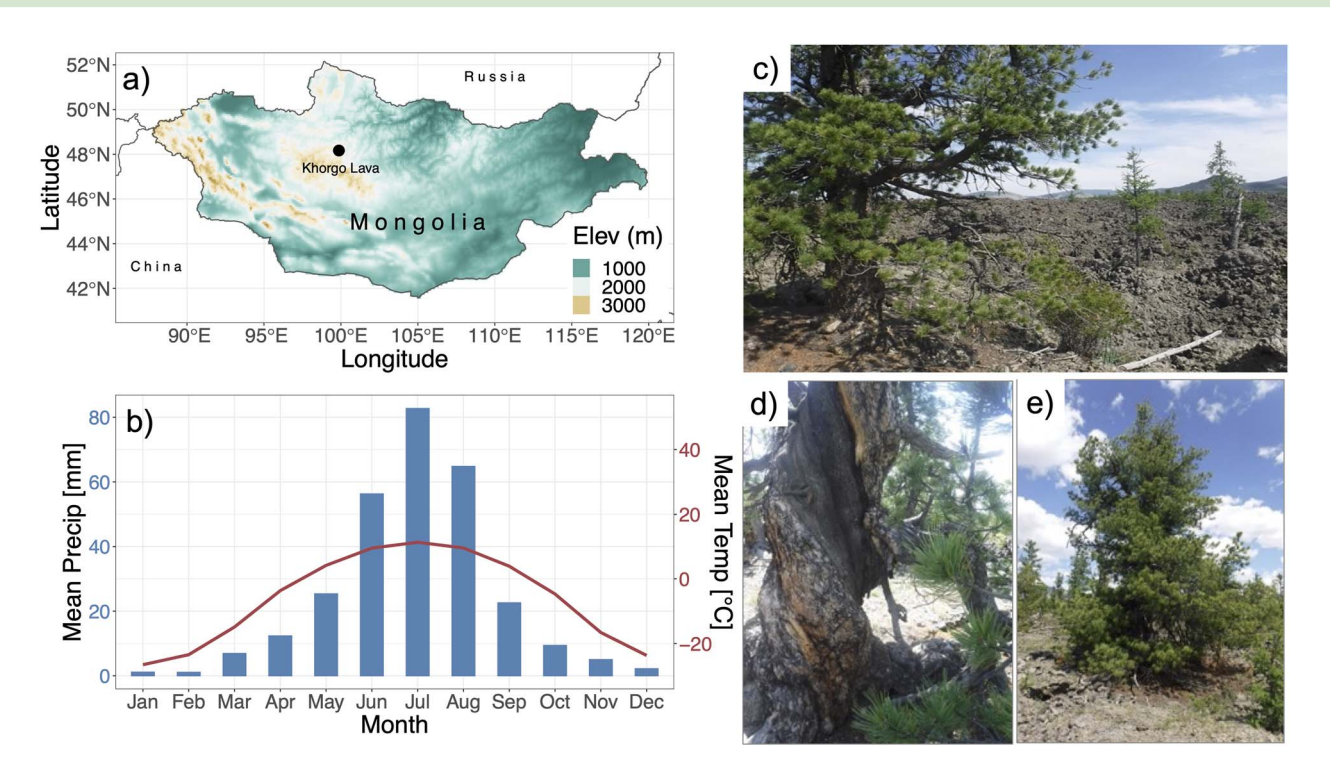


Figure 1. (a) An elevation map of Mongolia with the location of the study site (Khorgo Lava) shown as a black circle; (b) mean monthly precipitation (blue bars and left axis) and temperature (red line and right axis) near Khorgo Lava based on CRU version 4.01 from 1950 to 2011; (c) the Khorgo Lava study site where Siberian Pine and Siberian Larch trees are sparsely scattered on basaltic substrate; (d) an example of strip-bark morphology on a twisted Siberian Pine; (e) an example of a whole-bark Siberian Pine tree with a fully living stem and broad canopy.

Table 1. Analyzed tree-ring samples, their cambial status (strip-bark or whole-bark) and time span of ring-width record. An asterisk indicates that the core sample reached near pith. The column labeled Corr with KLP collection refers to correlations between each series and a larger collection of Khorgo Lava Siberian Pine samples (Leland et al. 2018). The percent of stem showing cambial dieback and the estimated dieback date (Leland et al. 2018), if available, are also provided for each strip-bark tree. Note that the estimated dieback date was based on a core from the dead stem portion of strip-bark trees and represents just 1 year, but it is likely that many dieback events occur through time as cambial dieback expands across the stem (Bunn et al. 2003, Leland et al. 2018).

Label	Sample ID	Cambial status	Time span (RW)	Corr with larger KLP collection	Percent of stem with dieback	Estimated dieback date
WB1	KLP0111	Whole	1627–2013	0.76	_	_
WB2	KPW036	Whole	1704-2014*	0.84	_	_
WB3	KPW077	Whole	1639-2014*	0.91	_	_
SB1	KLP058	Strip	1490-2011	0.78	Unknown	Unknown
SB2	KPS006	Strip	1662-2014	0.90	45%	1788
SB3	KPS037	Strip	1356–2014	0.83	57%	1853

dendrochronological procedures (Stokes and Smiley 1968). All cores were visually crossdated and compared against existing Khorgo Lava trees (different compilations in: Davi et al. 2006, Pederson et al. 2014, Leland et al. 2018, Hessl et al. 2018) and ring-widths (RW) were measured to 0.001 mm precision with a Velmex measuring system. There are high correlations between each ring-width series analyzed here and the master chronology from samples used in the recent Leland et al. (2018) compilation (Table 1; series correlations computed in the program COFECHA; Holmes 1983). The Leland et al. (2018) compilation was composed of a high number of samples

covering the last two centuries (138 series from 45 strip-bark and 35 whole-bark trees).

Here, we used detrended RW (RW $_{
m dt}$, i.e., dimensionless indices) to remove negative trends from raw RW data, especially evident in WB trees (Figure S1a, available as Supplementary data at *Tree Physiology* Online), associated with the increasing circumference of trees as they age (Fritts 1976). RW $_{
m dt}$ was calculated by taking the residuals of power-transformed ring-width series from fitted detrending curves (Cook and Peters 1997). We fit a negative exponential curve or linear function to each series, only allowing for a negative slope or horizontal line. All

detrending was performed in program ARSTAN (Cook and Krusic 2014). Though we opted for the 'residuals method' (Cook and Peters 1997), we compared RW $_{\rm dt}$ trends when calculating indices using the 'ratios method' (Fritts 1976). A robust mean of the detrended series was calculated to produce a mean RW $_{\rm dt}$ chronology for all six trees combined, and for SB and WB trees separately. We assessed the common signal between RW $_{\rm dt}$ records using the rbar (mean pairwise correlation between series) and the expressed population statistic (EPS; Wigley et al. 1984, a measure of how well a finite chronology represents a population signal).

Stable isotope records

Annual growth rings were cut from the increment cores using a scalpel under a stereoscope for the years 1830 to the most recent year of growth. We extracted α -cellulose from each ring to generate stable isotopic time series with annual resolution for each tree. The α -cellulose was isolated to prevent the effect of varying proportions of other wood components, such as lignin and hemicellulose, on stable isotope ratios of each sample (Loader et al. 2003). Wood from each year was subjected to chemical rinses of sodium hydroxide for solubilizing hemicelluloses and sodium chlorite/acetic acid for removing lignin (Loader et al. 1997, Andreu-Hayles et al. 2019). Chemicals were exchanged in individual filter tubes, in which each tube contained wood from a single year to prevent cross-contamination (Andreu-Hayles et al. 2019). The remaining α -cellulose was homogenized using an ultrasonic bath and freeze-dried, and then 200 μg ($\pm 10~\mu g$) of α cellulose were weighed from each ring and encapsulated in silver capsules for analysis.

The $\delta^{13}{\rm C}$ and $\delta^{18}{\rm O}$ were measured simultaneously through high-temperature pyrolysis of each sample into carbon monoxide using a High-Temperature Conversion Elemental Analyzer (TC/EA) interfaced with an isotope ratio mass spectrometer (IRMS) at the Lamont–Doherty Earth Observatory following methods described below and in Andreu-Hayles et al. (2019). The $\delta^{13}{\rm C}$ and $\delta^{18}{\rm O}$ ratios of each sample are expressed as delta (δ) values with reference to known standards, Vienna Pee Dee Belemnite (VPDB) for carbon and Vienna-Standard Mean Ocean Water (VSMOW) for oxygen, using the equations below.

$$\begin{split} \delta^{13}C_{sample} &= \left[\frac{(^{13}C/^{12}C)_{sample}}{(^{13}C/^{12}C)_{VPDB}} - 1\right] \times 1000 \\ \delta^{18}O_{sample} &= \left[\frac{(^{18}O/^{16}O)_{sample}}{(^{18}O/^{16}O)_{VSMOW}} - 1\right] \times 1000 \end{split}$$

To obtain these values, raw $\delta^{13}C$ and $\delta^{18}O$ were computed relative to CO reference gas (grade 4.7, Praxair) in the IRMS, and we then used a two-point calibration to correct raw $\delta^{13}C$

and $\delta^{18}O$ measurements using primary standards from the International Atomic Energy Agency (IAEA-CH6, IAEA-C3, IAEA-601 and IAEA-602). The precision of our measurements was assessed using the standard deviation of the primary standards: IAEA-CH6 (\pm 0.21) and IAEA-C3 (\pm 0.15) for δ^{13} C, and IAEA-601 (\pm 0.16) and IAEA-602 (\pm 0.37) for $\delta^{18}O$, as well as by an internal standard (Sigma Alpha cellulose; δ^{13} C: \pm 0.15, and $\delta^{18}O$: \pm 0.26).

Changes in the concentration and stable isotopic composition of atmospheric CO2 since industrialization have impacted the δ^{13} C of tree-ring cellulose in two ways. First, the gradual depletion in $\delta^{13}C$ of atmospheric CO_2 ($\delta^{13}C_{atm}$) due to the burning of fossil fuels is incorporated in tree-ring cellulose and imparts a decreasing trend in tree-ring $\delta^{\scriptscriptstyle 13} {\rm C}$ that is not related to physiological changes in the plant or its response to climate (i.e., the Suess Effect). To correct for the Suess Effect since 1850, we corrected the δ^{13} C tree-ring series (δ^{13} C_{corr}) by subtracting from each raw $\delta^{13}C$ tree-ring measurement the changes in $\delta^{13}C_{atm}$ from a preindustrial value (defined here as -6.6%) using the $\delta^{13}C_{atm}$ dataset from Belmecheri and Lavergne (2020). The so-called preindustrial (PIN) correction is often applied to remove changes in tree-ring $\delta^{13}C$ due to inferred physiological responses of plants to an increase in atmospheric CO₂ (McCarroll et al. 2009). Although the PIN correction is often used for paleoclimatic reconstructions, we sought to discern tree response to increasing atmospheric CO₂ concentrations and therefore did not apply this correction here. The individual $\delta^{\scriptscriptstyle 13} C_{\rm corr}$ and $\delta^{\scriptscriptstyle 18} O$ series were averaged together to produce a stable carbon and oxygen chronology for all sampled trees (n = 6), and for SB and WB trees individually (n = 3 trees per group). The common signal between treering series for all chronologies was evaluated using the rbar and

Climate sensitivity

We computed correlations of RW_{dt}, $\delta^{13}C_{corr}$ and $\delta^{18}O$ records with monthly climate variables to determine the sensitivities of the Siberian Pine trees to climate variability. Meteorological records in the region are sparse during the early 20th century and gridded climate products during that period can be less reliable, so only the period spanning from 1950 to 2011 (Figure 2a and b) was used here for climate analyses. Pearson correlation coefficients were calculated between the tree-ring parameters and monthly precipitation and average temperature from the Climatic Research Unit (CRU version 4.01) dataset (Harris et al. 2014), and a 3-month timescale Standardized Precipitation-Evapotranspiration Index (SPEI; Vicente-Serrano et al. 2010) from the grid point nearest to Khorgo Lava (48.25° N, 99.75° E; Figure 2a and b). Climate correlations were calculated using the RW_{dt}, δ^{13} C_{corr}, and δ^{18} O chronologies based on all six trees from this study. All climate correlations were computed in the R package 'treeclim' (Zang and Biondi 2015).

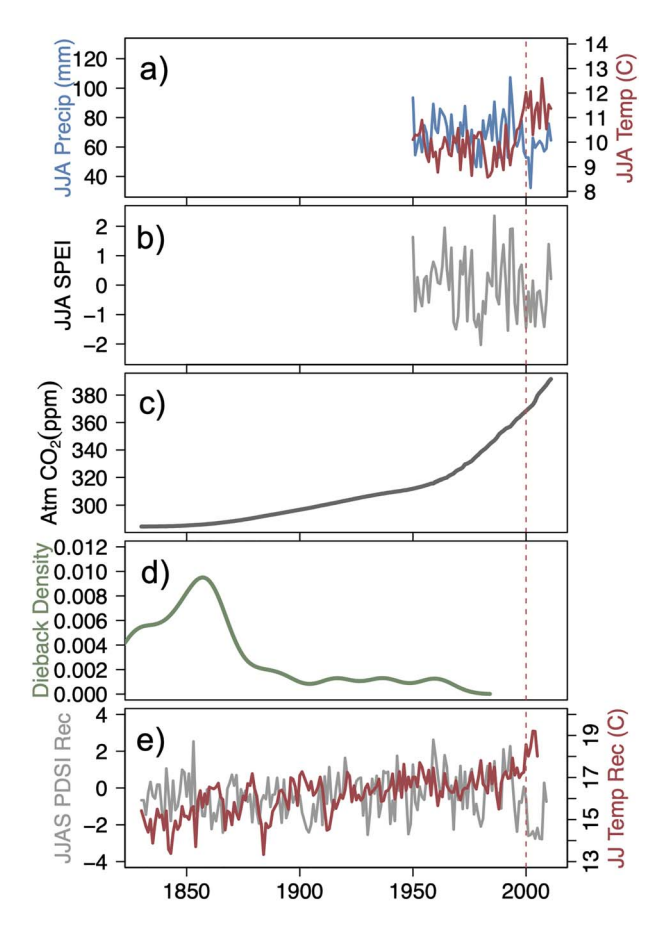


Figure 2. Climate and environmental records from 1830 to 2011 for the Khorgo Lava site. (a) June–August average CRU precipitation (blue) and temperature (red) and (b) SPEI-3 from a grid point nearest to Khorgo Lava; (c) atmospheric CO₂ concentrations derived from Robertson et al. (2001) until 1993, and then updated with mean annual values from Mauna Loa until 2011; (d) smoothed density estimates of dieback occurrence from strip-bark Siberian Pine at Khorgo Lava (Leland et al. 2018). (e) June–September self-calibrated Palmer's Drought Severity Index (scPDSI) reconstruction based on Siberian Pine from Khorgo Lava (gray; Pederson et al. 2014), and June–July temperature reconstruction from Northern Mongolia (red; Davi et al. 2015). The dashed line in all panels delineates the beginning of a significant drought period in central Mongolia (HessI et al. 2018).

Comparing strip-bark and whole-bark chronologies

We computed differences between SB and WB mean RW_{dt}, $\delta^{13}C_{corr}$ and $\delta^{18}O$ records from 1830 to 2011 to determine if the series diverged through time, as previously shown with ringwidth records from Khorgo Lava (Leland et al. 2018). A linear trend analysis was applied to the differenced series to determine if there was a significant diverging trend between SB and WB trees across each parameter through time.

Responses to atmospheric CO₂

We evaluated changes in intercellular CO_2 (c_i), the ratio of intercellular to atmospheric CO_2 (c_i/c_a), and intrinsic water-use efficiency (iWUE) over the full period of analysis (1830–2011) across all sampled trees. These parameters provide information

on gas-exchange in trees and are often used for estimating plant response to increasing c_a (Figure 2c). The raw (uncorrected) $\delta^{13}C$ values can be used to calculate c_i and c_i/c_a for each tree using a series of equations (Farquhar et al. 1982). First, we calculated carbon isotope discrimination against ^{13}C (Δ) as follows:

$$\Delta = \frac{\delta^{13}C_{\text{atm}} - \delta^{13}C_{\text{tree}}}{1 + \delta^{13}C_{\text{tree}}/1000}$$

Then, we applied the following equation:

$$\frac{c_i}{c_a} = \frac{\Delta - a}{b - a}$$

where the constant α represents fractionation associated with diffusion of CO₂ through stomata (4.4‰), and b is the discrimination against $^{13}CO_2$ by Rubisco during carboxylation (\sim 27‰). The average c_i and c_i/c_a ratio were calculated across all six trees from 1830 to 2011 and compared against simulated c_i and c_i/c_a values corresponding to three gas-exchange CO_2 response scenarios proposed by Saurer et al. (2004): (i) intercellular CO₂ concentration remains constant (constant c_i), (ii) intercellular CO2 increases proportional to atmospheric CO₂ concentration (constant c_i/c_a) and (iii) intercellular CO₂ increases parallel to atmospheric CO2 concentration (constant c_a-c_i). The simulations were initiated with an average of the first 5 years of c_i values (1830–1834), and then were extended to 2011, similar to methods implemented by Voltas et al. (2013). We applied the same method to the SB and WB groups separately. Growing season climate can also strongly influence $\delta^{\scriptscriptstyle 13}C_{corr},\;c_i/c_a,$ and iWUE through time. Therefore, due to the severity of the recent 21st century drought and its potential impact on the stable isotope records, we conducted the same analyses extending only to 1999.

To evaluate trends in iWUE from 1830 to 2011, we calculated the annual iWUE of individual trees (as below):

$$MUE = \frac{c_a \cdot (b - \Delta)}{1.6 \cdot (b - a)}$$

We assessed mean iWUE across all trees from 1830 to 2011, and we also compared mean iWUE of SB and WB trees. Similar to the analysis for RW_{dt}, $\delta^{13}C_{corr}$ and $\delta^{18}O$, we calculated differences between the mean SB and WB iWUE series through time and applied a linear trend analysis.

Results

Tree-ring data and trends

Tree-ring records within each parameter (RW_{dt}, δ^{13} C_{corr} and δ^{18} O) had a strong common interannual signal from 1830 to 2011, indicated by the rbar and EPS (Figures 3, S2 and S3, available as Supplementary data at *Tree Physiology* Online),

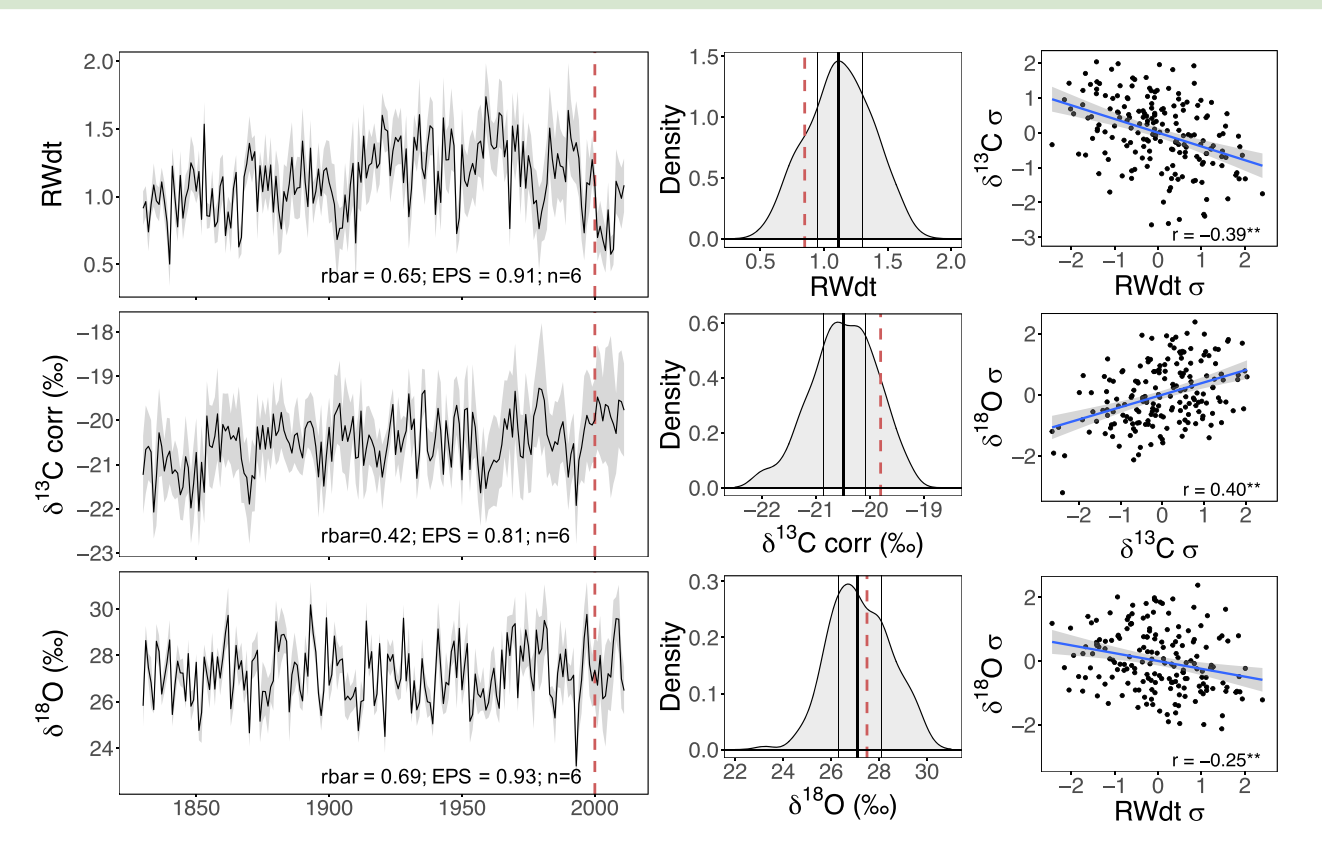


Figure 3. Left column: Annual detrended ring-widths (RW_{dt}), δ^{13} C corrected for the Suess Effect (δ^{13} C_{corr}) and δ^{18} O records from all six sampled trees (solid black line: mean; gray envelope: 95% confidence interval). The dashed red line indicates the beginning of a significant drought period at the turn of the 21st century (Hessl et al. 2018). Middle column: Probability density functions of each parameter from 1830 to 2011. The solid vertical lines represent the 25th, 50th (bold) and 75th percentile of each dataset, and the red dashed line indicates the mean of the drought period from 2000 to 2011. Right column: The relationship between normalized parameters (blue: regression line; gray: 95% confidence interval) with the respective correlations shown on the bottom right. ** indicates significance at P < 0.01.

with RW_dt and $\delta^{\mbox{\tiny 18}} \mbox{O}$ records showing the strongest agreement (Table 2). The RW_{dt}, $\delta^{13}C_{corr}$ and $\delta^{18}O$ tree-ring chronologies were significantly correlated with one another from 1830 to 2011 (RW_{dt} vs. δ^{13} C_{corr}: r = -0.39; P < 0.01; δ^{18} O vs. $\delta^{13}C_{corr}$: r = 0.40; P < 0.01; RW_{dt} vs. $\delta^{18}O$: r = -0.25; P < 0.01; Figure 3). Due to a lower sample size, individual SB and WB chronologies (n = 3 trees per group) had a weaker common signal, especially with respect to the $\delta^{13}C_{corr}$ parameter (Table 2). Furthermore, the WB group had a large $\delta^{13}C_{corr}$ range of values (Figure 4), as WB2 had notably depleted $\delta^{\scriptscriptstyle 13} C_{\rm corr}$ values relative to other WB trees (Figure S2, available as Supplementary data at Tree Physiology Online). However, mean SB and WB chronologies showed similar interannual variability across all parameters (Figure 4). The SB and WB mean chronologies are significantly correlated (P < 0.01) with r = 0.74 for RW_{dt}, r = 0.70 for δ^{13} C_{corr} and r = 0.88 for δ^{18} O from 1830 to 2011.

Regarding long-term trends, the SB mean chronologies increased relative to the WB chronologies for all three parameters, and the linear trend of differences between SB and WB chronologies was significant in all cases (P < 0.01; Figure 4). This divergence between SB and WB RW_{dt} occurs regardless of using the ratios or residuals method of standardization

(Figure S1b and c, available as Supplementary data at *Tree Physiology* Online). The smaller sample set used here captures long-term mean SB and WB RW_{dt} differences observed from the larger Leland et al. (2018) collection of trees (Figure S4, available as Supplementary data at *Tree Physiology* Online). Given the large range of values across individuals from each parameter, particularly with respect to the $\delta^{13}C_{corr}$ dataset, we tested this analysis after normalizing all tree-ring series before producing mean chronologies and the same significant trend differences were obtained (Figure S5, available as Supplementary data at *Tree Physiology* Online).

On an individual-tree level, all SB trees showed a higher trend in RW_{dt} relative to WB trees, and most (two out of three) SB trees showed higher trends in $\delta^{13}C_{corr}$ compared with WB trees from 1830 to 2011 (Figure S3, available as Supplementary data at *Tree Physiology* Online). When excluding the recent drought (i.e., comparing trends from 1830 to 1999), all SB trees had a higher increasing $\delta^{13}C_{corr}$ trend relative to WB trees. This is because WB1 showed a strong enrichment associated with the 21st century drought that had an impact on its long-term trend (Figure S2, available as Supplementary data at *Tree Physiology* Online). Although the $\delta^{18}O$ of SB trees increased

Table 2. Measures of common signal strength between series. The mean correlation between series (rbar) and expressed population signal (EPS) were calculated for each subset (all trees, strip-bark (SB) and whole-bark (WB)), and for each parameter (detrended ring-width (RW_{dt}), and stable carbon ($\delta^{13}C_{corr}$) and oxygen ($\delta^{18}O$) isotopes).

Subset	# Samples	RW _{dt}		$\delta^{13}C_corr$		δ^{18} O	
		rbar	EPS	rbar	EPS	rbar	EPS
All	6	0.65	0.91	0.42	0.81	0.69	0.93
SB	3	0.68	0.86	0.43	0.70	0.67	0.86
WB	3	0.69	0.87	0.38	0.65	0.71	0.88

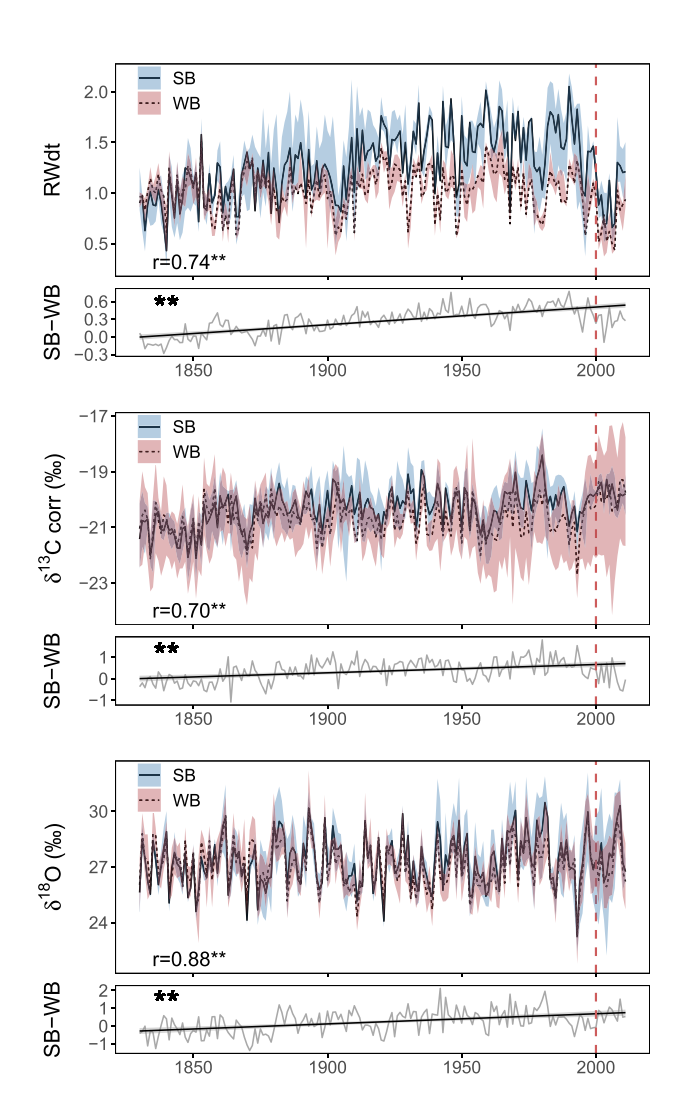


Figure 4. Detrended ring-widths (RW_{dt}), δ^{13} C corrected for the Suess Effect ($\delta^{13}C_{corr}$) and $\delta^{18}O$ chronologies from strip-bark and whole-bark trees. The solid (dotted) line is the mean of the strip-bark (whole-bark) series, and the blue (red) envelope represents the full range of values across all three sampled trees. The plots below the mean chronologies show the difference between strip-bark and whole-bark values over time for each parameter (gray; SB–WB) and are accompanied with a black linear trend line (significance denoted with **P < 0.01). The dashed red line in each plot indicates the beginning of a significant drought period at the turn of the 21st century (Hessl et al. 2018).

on average relative to WB trees, the individual $\delta^{18}{\rm O}$ records showed higher variability in trends: in particular, SB2 showed

a significant δ^{18} O declining trend (P < 0.05) whereas the other SB trees significantly increased from 1830 to 2011 (P < 0.05; Figure S2 and Figure S3, available as Supplementary data at *Tree Physiology* Online).

Responses to climatic variability

The RW_{dt}, $\delta^{13}C_{corr}$ and $\delta^{18}O$ chronologies based on all analyzed trees (Figure 3) showed strong sensitivity to climate during the current-year growing season, particularly during June through September, as well as sensitivity to some months of the previous-year growing season (Figure 5). The RW_{dt} chronology had a significant positive correlation to current-year June and July precipitation (r=0.52 and r=0.27; $P\leq0.05$), and a significant negative correlation to temperature during June–August (r=-0.57, -0.53 and -0.34, respectively, P<0.05). RW_{dt} showed significant sensitivity to SPEI-3 for a more extended season, from June through September, and the correlation between RW_{dt} and the average SPEI-3 of those months was highly significant (r=0.51, P<0.05). A weaker sensitivity to moisture conditions (SPEI-3) during the prior-year growing season was also evident.

The $\delta^{13}C_{corr}$ chronology had a significant and negative correlation with precipitation and a positive correlation with temperature, especially during June and July (precipitation: r=-0.56, -0.45 (P<0.05) and temperature: r=0.50 and 0.48, P<0.05). There was also a strong negative correlation between $\delta^{13}C_{corr}$ and June through September average SPEl-3, (r=-0.55, P<0.05). In agreement with a relationship between drought variability and $\delta^{13}C_{corr}$, there was an enrichment in mean $\delta^{13}C_{corr}$ during the 21st century drought; average $\delta^{13}C_{corr}$ from 2000–2011 (also defined by higher atmospheric CO_2 levels) was above the 75th percentile of all $\delta^{13}C_{corr}$ chronology values (Figure 3, middle column). The $\delta^{13}C_{corr}$ enrichment was concurrent with a decrease in RW_{dt} below the 25th percentile during the 21st century drought (Figure 3, middle column).

Although the $\delta^{18}O$ chronology was significantly and negatively correlated with average June through September SPEl-3 (r=-0.41, P<0.05), these correlations were weaker than those calculated for RW_{dt} and $\delta^{13}C_{corr}$. The mean $\delta^{18}O$ during the 21st century drought was slightly enriched (i.e., above the 50th percentile of all $\delta^{18}O$ chronology values), but

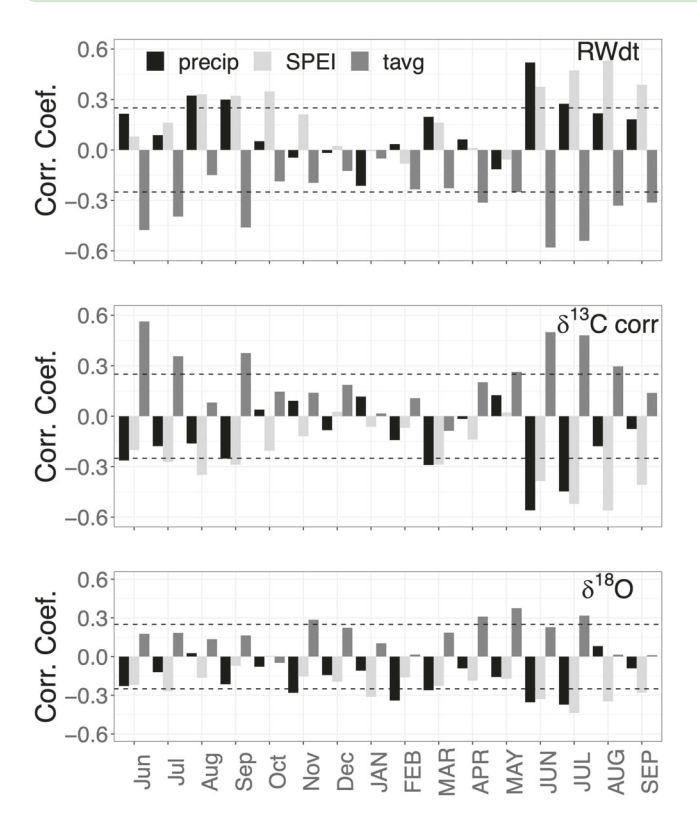


Figure 5. Pearson's correlation coefficients between RWdt (top), $\delta^{13}C_{corr}$ (middle) and $\delta^{18}O$ (bottom) chronologies derived from all trees and monthly climate variables from 1950 to 2011. Tree-ring data were compared against CRU TS 4.01 precipitation (precip; black), CRU TS 4.01 average temperature (tavg; medium gray) and 3-month SPEI (light gray). Months with lower case lettering refer to correlations with the year prior to the current year of growth, and the months with capital lettering refer to the current year of growth. Correlation coefficients exceeding the gray dashed lines are statistically significant (P < 0.05).

the response was not as pronounced compared with $\delta^{13}C_{corr}$ and RW_{dt} (Figure 3, middle column). However, unlike the other treering parameters, the $\delta^{18}O$ chronology had a stronger sensitivity to spring temperature, with significant and positive correlations to April and May temperatures (r=0.33 and 0.38, P<0.05).

Intercellular CO₂ concentration and iWUE trends

There was a mean increase in intercellular CO_2 concentration (c_i) from 1830 to 2011 based on all trees (Figure 6); this increase falls between the simulation of constant c_i/c_a (Scenario 2) and constant c_i (Scenario 1), with a slightly closer association with the latter (simulated c_i vs. measured c_i RMSE = 12.44 for Scenario 1 and 12.49 for Scenario 2; simulated c_i/c_a vs. measured c_i/c_a RMSE = 0.037 for Scenario 1 and 0.039 for Scenario 2; Figure 6, Table S1 available as Supplementary data at *Tree Physiology* Online). The average of SB trees alone was more closely associated with constant c_i (Scenario 1), whereas the WB trees fell closest to a constant c_i/c_a (Scenario 2; Table S1 available as Supplementary data at *Tree Physiology* Online), as shown in Figure 7. The WB trees maintained a relatively constant c_i/c_a throughout the entire record, until a large mean decline

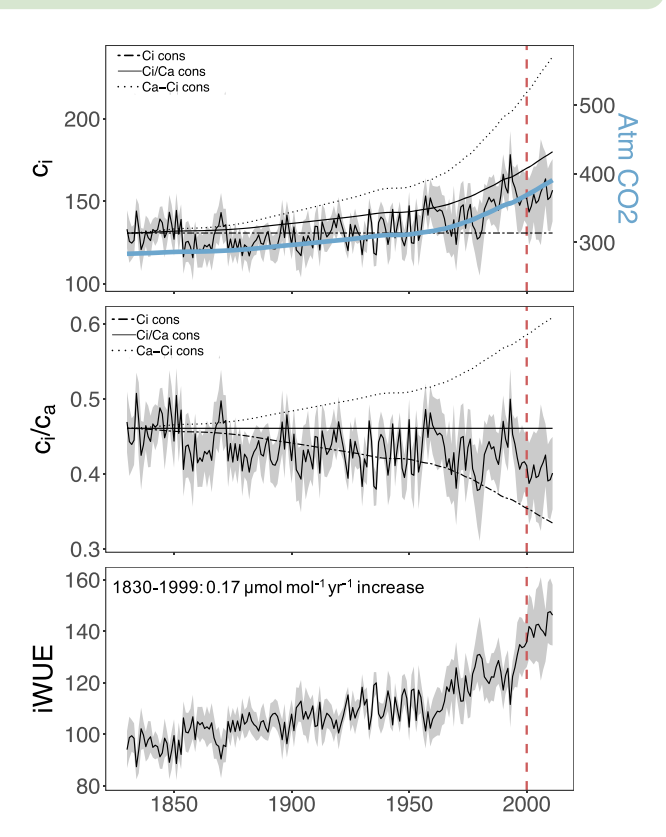


Figure 6. Top: Mean intercellular CO_2 (c_i) across all analyzed trees, with 95% confidence interval in gray and compared with simulations following the three scenarios proposed by Saurer et al. (2004). The blue line indicates changes in atmospheric CO_2 (c_a , right axis). Middle: Mean ratio of intercellular to ambient CO_2 (c_i/c_a) with 95% confidence interval in gray shading, also compared with simulations following the three scenarios proposed by Saurer et al. (2004). Bottom: Mean intrinsic water-use efficiency (iWUE) across all analyzed trees with the 95% confidence interval highlighted in gray. The dashed red line indicates the beginning of a significant drought period at the turn of the 21st century (Hessl et al. 2018).

during the 21st century drought (but large variance), while the SB trees exhibited a longer-term decline in c_i/c_a , particularly notable in the 19th century (Figure 7). The same scenario was tracked by each group when testing only the years 1830–1999, preceding the severe drought of the 2000s (Table S1 available as Supplementary data at *Tree Physiology* Online).

The average iWUE of all trees increased by 0.21 μ mol mol⁻¹ yr⁻¹ from 1830 to 2011 and 0.17 μ mol mol⁻¹ yr⁻¹ from 1830 to 1999, excluding the most recent severe drought (Figure 6). During the 20th century alone, comparing the mean from 1900–1909 to 1990–1999, the average iWUE at our study site increased by 16.19%. Refer to Table S2 available as Supplementary data at *Tree Physiology* Online for detailed information on mean iWUE changes for different periods of time and comparisons with the literature. Similar to other comparisons, SB and WB trees also showed differences in long-term iWUE. There was a positive and significant trend in the difference between SB mean iWUE relative to WB trees from 1830 to 2011 (P < 0.01; Figure 7).

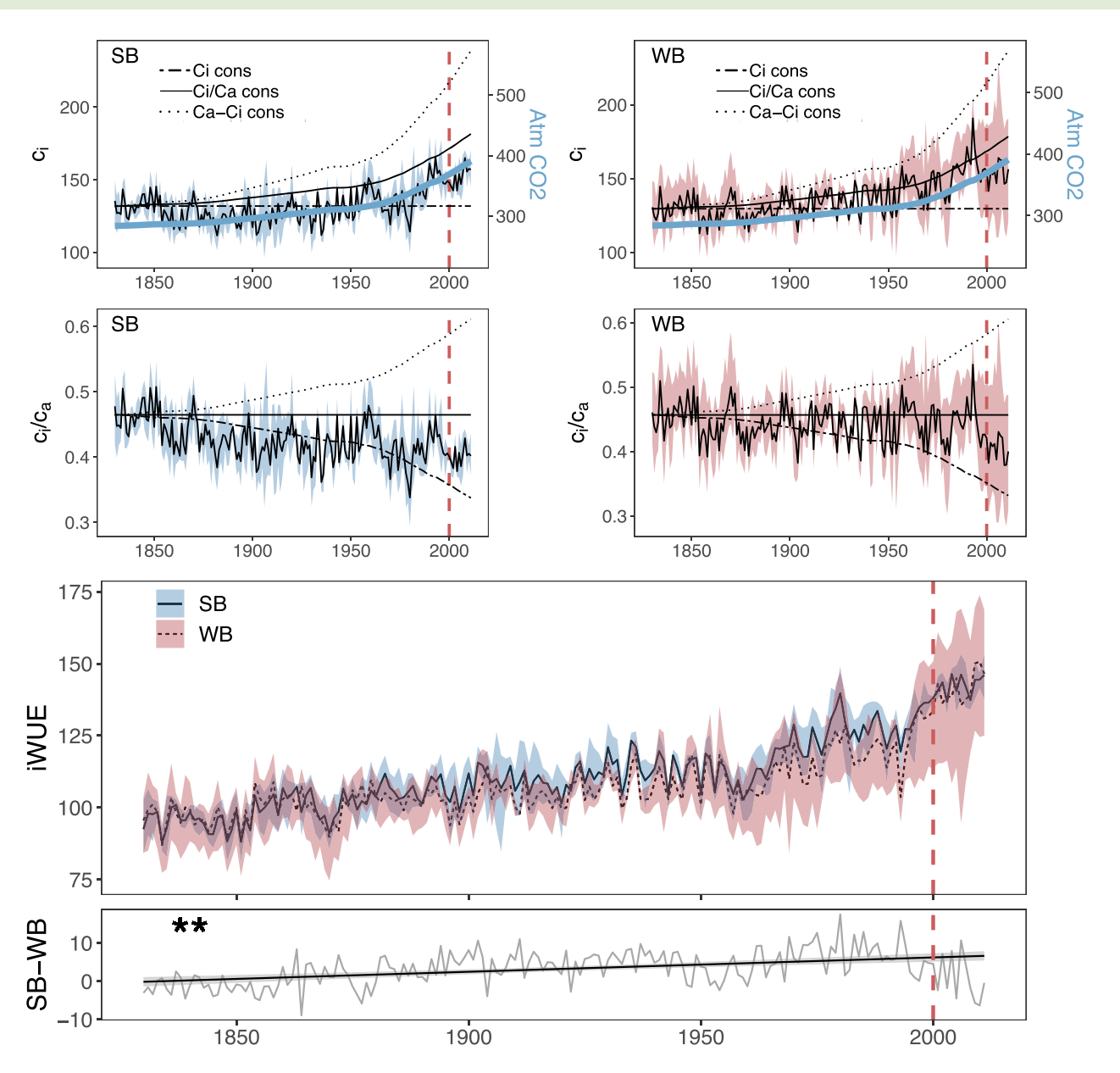


Figure 7. Top: Mean intercellular CO_2 (c_i) across SB (left) and WB (right) trees, with the range of values represented in blue and red shading, respectively. The c_i are compared with simulations following the three scenarios proposed by Saurer et al. (2004). The blue line indicates changes in atmospheric CO_2 (c_a , right axis). Middle: The same as the top row, but illustrating changes in mean c_i/c_a over time. Bottom: Mean intrinsic water-use efficiency (iWUE) across SB (solid) and WB (dotted) trees with the range highlighted in blue and red, respectively. The plot below mean iWUE shows the difference between strip-bark and whole-bark iWUE values over time (gray; SB–WB), accompanied with a black linear trend line (**P < 0.01).

Discussion

The 182-year tree-ring stable isotopic records presented here provide insight on the physiological responses of trees to climatic and environmental conditions in north-central Asia. Our results show that tree-ring $\delta^{13}C$ and $\delta^{18}O$ in Siberian Pine from the Khorgo Lava field, a xeric site in arid central Mongolia, are sensitive to interannual moisture availability during summer months. The tree-ring $\delta^{18}O$ record also partially reflects

interannual variability in spring temperatures. Over the long-term, the trees showed an intermediate response between two different gas-exchange strategies, maintaining a constant intercellular CO_2 (c_i) or constant ratio of intercellular to ambient CO_2 (c_i/c_a). However, we also found a divergence in mean treering stable isotopic trends of different stem morphologies, which suggests that partial cambial dieback may be associated with different leaf-level physiological behavior.

Climatic controls on ring-width and tree-ring stable isotope records

We found significant positive correlations between ring-width at Khorgo Lava and precipitation and SPEI-3 during summer months (June-July for precipitation, and June-September for SPEI-3). These results are in agreement with earlier studies finding a strong relationship between Khorgo Lava tree-ringwidths and another drought index, the self-calibrating Palmer Drought Severity Index (scPDSI), for the months of June through September (Pederson et al. 2014, Hessl et al. 2018). In addition, we found that both $\delta^{13} C_{corr}$ and $\delta^{18} O$ are correlated with summer hydroclimate and temperature, with enriched values during dry/hot years and depleted values during wet/cool years. The pronounced decrease in mean ring-width and increase in mean $\delta^{13}C_{corr}$ during the recent, severe drought starting at the turn of the 21st century (Figure 3), also illustrates the significance of moisture availability on the physiology of Siberian Pine at this site.

The summertime drought sensitivities of ring-width, $\delta^{13}C_{corr}$ and δ^{18} O, as well as the significant, positive correlations between $\delta^{13}C_{corr}$ and $\delta^{18}O$, indicate that changes in stomatal conductance likely play an important role in tree-ring stable isotope variability at Khorgo Lava. Positive correlations between $\delta^{13}C_{corr}$ and $\delta^{18}\text{O}$ can occur because drier (low humidity) conditions, in addition to low water supply, are associated with both stomatal closure and leaf water enrichment (e.g., Saurer et al. 1997a, Andreu-Hayles et al. 2022). A combined analysis of changes in $\delta^{13}C_{corr}$ and $\delta^{18}O$ (the 'dual-isotope approach') has been used to disentangle the primary driver of $\delta^{13}C_{corr}$ variability (i.e., assimilation or stomatal conductance), under the assumption that δ^{18} O variability is primarily influenced by transpiration rates and that source water remains constant (Scheidegger et al. 2000, Roden and Siegwolf 2012). Applying this concept here (though see important caveats and cautions regarding source water in the δ^{18} O description below), the positive relationship between $\delta^{13}C_{corr}$ and $\delta^{18}O$ records (Figure 3), and the sensitivity of these parameters to summer drought, suggest that stomatal regulation is likely an important driver of variability in stable carbon isotopes at Khorgo Lava. Such a relationship between $\delta^{13}C_{corr}$ and $\delta^{18}O$ has been described in other studies, especially in dry sites or during water-limited periods (e.g., Sidorova et al. 2009, Liu et al. 2014, Rodriguez-Caton et al. 2021). Negative correlations between $\delta^{13}C_{corr}$ and RW_{dt} further suggest that both stomatal conductance and radial growth decrease under dry conditions (Saurer et al. 1997b). Although stable carbon isotopes and ring-width records are correlated here, they are related to different physiological processes (i.e., carbon uptake at leaf-level and xylogenesis), which can be decoupled (Andreu-Hayles et al. 2022). As drought conditions reduced RW_{dt} and increased $\delta^{13}C_{corr}/\delta^{18}O$, it is likely that both processes are limited by moisture availability at our study site. Research suggests that over large scales, tree growth is largely limited

by cambial activity (a 'sink' limitation, impacted by limiting environmental factors, such as drought) rather than carbon assimilation through photosynthesis (Cabon et al. 2022).

The δ^{18} O chronology has a more complex climate signal relative to $\delta^{13}C_{corr}$, which could reflect the various factors that influence the $\delta^{18}O$ of leaf water and tree-ring cellulose. Treering $\delta^{18}O$ had a weaker, though still significant, response to summer hydroclimate (especially precipitation and SPEI-3) than the other parameters. More enriched $\delta^{18} O$ during drier years is most likely associated with evaporative enrichment at the leaf-level or soil water evaporation altering the $\delta^{18}\mathrm{O}$ of source water for the trees (Roden et al. 2000, McCarroll and Loader 2004), especially considering the xeric conditions of the study site . Accordingly, the $\delta^{18} \text{O}$ chronology showed weak though significant positive correlations with growing season summer temperatures in July, as well as significant and negative correlations with June and July precipitation and SPEI-3. In contrast, during the spring (April and May), significant δ^{18} O correlations were found with temperature, which might reflect the importance of temperature on regional precipitation δ^{18} O. There is a strong, positive relationship between δ^{18} O of precipitation and air temperature (Dansgaard 1964) that is clearly evident at high latitudes in the northern hemisphere (Birks and Edwards 2009), including portions of northern Asia (Araguás-Araguás et al. 1998, Yamanaka et al. 2007). This temperature effect on precipitation δ^{18} O has been found to leave an imprint on tree-ring cellulose δ^{18} O in various high-latitude forests (e.g., Saurer et al. 2002, Porter et al. 2014, Field et al. 2021, Gagen et al. 2022). Similar δ^{18} O climate responses in the spring and summer months were identified in Siberian Pine growing in the Russian Altai in southern Siberia (Loader et al. 2010) suggesting that both regional precipitation δ^{18} O (influenced partly by temperature) and leaf-level processes related to humidity might be important regional drivers of tree-ring δ^{18} O.

Additional factors that could influence precipitation $\delta^{18} {\rm O}$ in Mongolia and ultimately the $\delta^{18} O$ of cellulose include the proportion of local moisture recycling, a significant contributor to precipitation in arid central and northern Asia (Wang et al. 2016), or water source changes, including changes in largescale atmosphere circulation (Vuille et al. 2005, Liu et al. 2009, Wang et al. 2020, Kang et al. 2022). An analysis of precipitation δ^{18} O suggests that water vapor in Mongolia is largely transported by the westerlies during the summer, with limited contributions from southerly (monsoonal) sources (Sato et al. 2007). However, Mongolia is neighboring regions impacted by monsoonal systems, and some studies have found linkages between tree-ring $\delta^{18}O$ and monsoonal variability in the summer, as well as relative humidity, in north China (Liu et al. 2019, Wang et al. 2020a, Xu et al. 2021). The degree to which differing climate (source water) systems have impacted precipitation δ^{18} O in the Khorgo Lava region, and their potential time-varying properties over the last several centuries, will be

important to investigate in relation to tree-ring $\delta^{18}O$ in future studies. Furthermore, the Khorgo Lava field appears to have a complex underlying hydrology, with some trees potentially accessing the water table at different times, or taking up water from deeper pools. This variation could impact the source water δ^{18} O signature of individual trees (e.g., Sarris et al. 2013) and could not be accounted for here. Although the common signal between δ^{18} O records from all trees was particularly strong, suggesting that microsite plays a negligible role in interannual δ^{18} O variability, long-term δ^{18} O trends differed between some trees (Figure S3, available as Supplementary data at Tree Physiology Online). All of the factors potentially impacting source water through time, either across all trees or for individual trees, complicate the dual-isotope interpretation for assessing $\delta^{13} C$ variability above (Roden and Siegwolf 2012). However, given the extreme aridity of central Mongolia, it is likely that relative humidity and its impact on leaf-level processes has continually contributed to variability in tree-ring δ^{13} C and δ^{18} O at Khorgo Lava.

The sensitivity of the Siberian Pine stable isotope records to climatic variability shown here indicates that these tree-ring parameters hold significant paleoclimate potential. The $\delta^{13} \mathrm{C}$ and δ^{18} O records can either complement tree-ring width datasets in climate reconstruction or provide additional/multidimensional climate information. As the δ^{13} C and δ^{18} O records partly reflect summer hydroclimate, they could be used to reinforce our understanding of past hydroclimate based on ring widths. Furthermore, the unique sensitivity of δ^{18} O could provide insights on past spring temperature variability or potentially, changes in large-scale circulation patterns and shifts in precipitation δ^{18} O (e.g., Szejner et al. 2016, Field et al. 2021). An understanding of variations in δ^{18} O of precipitation in Mongolia (e.g., Sato et al. 2007, Yamanaka et al. 2007) and their impact on δ^{18} O of treering cellulose in Mongolia, especially over decadal and longer time scales, should be investigated further if this metric is to be employed for dendroclimatology.

Leaf gas-exchange strategies and iWUE trends

The Khorgo Lava trees fell between two scenarios of stomatal regulation of gas-exchange described in the literature: a constant ratio of intercellular to ambient CO_2 (c_i/c_a) and a constant intercellular CO_2 (c_i). A constant c_i/c_a indicates that intercellular CO_2 increases proportionally with ambient CO_2 , suggesting a moderate increase in iWUE associated with a moderate decrease in stomatal conductance and/or an increase in assimilation. A constant intercellular CO_2 corresponds to a larger increase in iWUE relative to the constant c_i/c_a scenario. These two scenarios of leaf gas-exchange strategies, in addition to a constant c_a-c_i scenario (a 'passive' response with a weak regulation of stomatal conductance with increasing CO_2), have been reported in the literature. However, a constant c_i/c_a is the prevailing strategy reported across different tree-ring studies (e.g.,

Saurer et al. 2004, Frank et al. 2015) and most free-air carbon dioxide enrichment (FACE) experimental studies (Lavergne et al. 2019). Our results, therefore, are consistent with other studies suggesting an 'active response' to increasing atmospheric CO_2 , with a corresponding increase in iWUE.

However, the intermediate response between the constant c_i/c_a and constant c_i scenarios based on the average of all trees in our study (Figure 6) partly reflects diverging trends between strip-bark and whole-bark trees (Figure 7). The whole-bark trees more consistently followed the constant c_i/c_a scenario, while the strip-bark trees had a statistically closer association with the constant c_i scenario. However, it is important to note that trees might not employ a single leaf gas-exchange strategy through time; rather, these strategies can be dynamic with increasing atmospheric CO_2 in order to maximize carbon gain and reduce water loss (Voelker et al. 2016, Giguère-Croteau et al. 2019, Marchand et al. 2020, Belmecheri et al. 2021). Strip-bark c_i/c_a appears to be particularly dynamic over time, with a step-change decline in mean c_i/c_a occurring around the mid-to-late 1800s that was not evident in whole-bark trees (Figure 7).

The rate of iWUE increase in Siberian Pine during the 19th and 20th centuries at Khorgo Lava (Figure 6) was within the range of increasing iWUE reported in several studies throughout Asia and Europe (Table S2 available as Supplementary data at Tree Physiology Online). For example, from 1900 to 2006, Huang et al. (2017) reported a general iWUE increase of 27.83% in Smith Fir from the Tibetan Plateau, similar to a 30.66% increase from the Khorgo Pine for that same period. The iWUE averaged across all trees increased by 17.17% from the 1861-1890 mean to 1961-1990 mean, compared with an iWUE increase of 19.2 \pm 0.9% in other conifers from Eurasia (Saurer et al. 2004). A more recent study found that conifers in Europe showed a 25.7% \pm 11.6% iWUE increase when comparing the 1901-1910 mean with the 1991-2000 mean (Saurer et al. 2014), compared with an 18.43% average iWUE increase at Khorgo Lava during that time. Although the average iWUE trend found here was similar to that of many other regional conifers, the iWUE trends between strip-bark and whole-bark trees also diverged through time, with a steeper increase in stripbark iWUE (Figure 7). This finding supports the notion that there are several possible drivers of increasing iWUE at the tree level, such as environmental and developmental factors, in addition to the leaf-level physiological responses to increasing atmospheric CO₂ (e.g., Marchand et al. 2020). Furthermore, climate impacts on stable carbon isotopes can play an important role in shortterm variability and long-term iWUE trends (Frank et al. 2015). Regarding the 21st century drought, while removal of the post-1999 period did not alter the scenarios of stomatal regulation of gas-exchange tracked by the trees in general, high evaporative demand during that period likely contributed to the observed step-change increase in mean iWUE at the turn of the century (Figures 6 and 7).

Tree morphology and diverging long-term trends

Strip-bark and whole-bark trees showed similar interannual variability in ring-width and stable isotope records, but their long-term trends differed over the last two centuries. Strip-bark trees trended towards larger ring-widths relative to whole-bark trees over the last two centuries at Khorgo Lava (Leland et al. 2018), as has been described in two other species (Bunn et al. 2003, Ababneh 2006). Although some detrending methods can artificially inflate differences in ring-widths between the two morphological groups (Salzer et al. 2009), the diverging trends over the last two centuries are apparent in both mean raw ring-width and standardized chronologies at Khorgo Lava (Figure S1, available as Supplementary data at Tree Physiology Online; Leland et al. 2018) and are therefore not an artifact of dendrochronological methods. Importantly, an increasing ringwidth trend in strip-bark trees does not necessarily mean stripbark trees are adding more radial growth than whole-bark trees; it is possible that a similar or smaller amount of radial growth is added to a smaller active stem area on strip-bark trees. The everchanging stem and canopy area of strip-bark individuals makes overall radial growth comparisons between strip-bark and whole-bark trees difficult to quantify.

In addition to diverging ring-width trends, this study found that strip-bark trees also trended towards higher mean $\delta^{\scriptscriptstyle 13}{\rm C}$ and δ^{18} O values, and a higher mean iWUE over time, relative to whole-bark trees. This finding contrasts with results from Tang et al. (1999), in which there was no significant difference in the iWUE trends of two whole-bark (or 'full-bark') and two strip-bark Bristlecone Pine from 1795 to 1995. Our results of diverging iWUE trends remain consistent when restricting our analyses to the 1830-1995 period (Figure S6, available as Supplementary data at Tree Physiology Online), to match the final year of the Tang et al. (1999) study, suggesting that the most recent years did not drive the differences we identified. In the Tang et al. (1999) study, it was hypothesized that increases in iWUE could be similar between strip-bark and whole-bark trees, but differences in carbon petitioning could contribute to differing ring-width trends. The reasons as to why we observe different results than Tang et al. (1999) regarding iWUE trends in strip-bark and whole-bark trees is uncertain, but it could be related to different physiological behavior of tree species, and/or the timing and degree of cambial dieback events, among other factors. Importantly, in this study, we analyzed strip-bark trees with clear increasing ring-width trends (relative to wholebark trees) for comparison with their stable isotope records. Our contrasting results underscore that trends in various treering parameters from strip-bark and whole-bark trees should be further explored across different species and sites. Furthermore, we recommend that future studies analyze tree-ring stable isotopes from a large number of strip-bark trees with differing degrees of cambial dieback or radial growth trends. Differing stable isotopic trends could have important implications for

climate reconstructions derived from long-lived trees prone to partial cambial dieback.

Although the mechanisms behind diverging stable isotope trends of strip-bark trees at Khorgo Lava remain uncertain, size and developmental changes in trees can impact stable isotope records and iWUE trends (e.g., Brienen et al. 2017, Klesse et al. 2018, Marchand et al. 2020). The dual-isotope model (Scheidegger et al. 2000), taking into consideration the source water assumptions described earlier (Roden and Siegwolf 2012), suggests that simultaneously increasing δ^{13} C and δ^{18} O of stripbark relative to whole-bark trees could indicate a trend towards reduced stomatal conductance in strip-bark trees over time. Interestingly, a large decrease in strip-bark mean intercellular CO₂ was observed in the mid-1800s perhaps related to a shift towards more conservative stomatal behavior. This occurred after an extensive dieback event that was observed in estimated dieback dates (Figure 2d) following a cold and dry period in Mongolia in the 19th century (Figure 2e and described in Leland et al. 2018). One hypothesis is that stem dieback results in a higher leaf area relative to the now-reduced stem area, leading to larger radial growth measurements on the living portion of the stem but a decrease in stomatal conductance (Voltas et al. 2013, Gessler et al. 2018). While we do not know the extent to which all the individual strip-bark trees in this study experienced stem dieback in the 1800s, it is conceivable that this period could have played a role in the ring-width and stable isotope trends of strip-bark trees described here. Interestingly, a notable shift towards higher ring-width and $\delta^{13}C_{corr}$ (lower ci and c_i/c_a), and a higher δ^{18} O, was observed specifically in the SB3 tree after an estimated dieback event in the year 1853 (Figure S7, available as Supplementary data at Tree Physiology Online). This single-tree result, however, should be taken with caution. This was the only tree with an estimated dieback event during the period of analysis in this study, and there are uncertainties in actual dieback dates given possibilities of degradation of the dead portion of the stem over time (Leland et al. 2018).

Although the strip-bark and whole-bark comparisons from this study are based on a limited number of samples, our study illuminates differences in ring-width and stable isotopes trends of the two morphological types, warranting future physiological work to continue studying this phenomenon. Determining the drivers behind these trends will require information about the degree of sectored architecture of strip-bark trees (Larson et al. 1993), the relation between canopy and stem/sapwood area, and leaf-level physiological responses following stem dieback events. Here, we studied leaf-level iWUE derived from tree-ring stable carbon isotopes, though whole-plant WUE (i.e., a measure of dry matter production per unit of water loss) could also differ between strip-bark and whole-bark trees and could not be assessed here. We also found some variability in individual-tree trends within strip-bark and whole-bark groups; whereas

the trends between individuals within each morphological group largely agreed, the decreasing $\delta^{18}O$ trend of SB2 notably contrasted with the large positive trend of other strip-bark trees, perhaps reflecting microsite conditions, water source and/or developmental stage of that individual. These results highlight the importance of a high sample depth, as well as analyzing individual trees for stable isotope analyses (vs. pooling from multiple trees), to identify and explain potential differences between trees with differing morphological traits.

Conclusions

This study highlights the sensitivity of Siberian Pine $\delta^{\scriptscriptstyle 13}{\rm C}$ and $\delta^{18}\text{O}$ tree-ring records to climate variability during the instrumental era, and provides insight on the gas-exchange behavior of long-lived trees growing on a xeric site. Although the stable carbon and oxygen isotopes have a similar summer hydroclimate (moisture) signal as the ring-width chronologies during the instrumental era, the stable oxygen isotope records display a more complex signal that could additionally provide information about spring temperature. Comparisons of stripbark and whole-bark chronologies suggests that there are differences between stem morphological types in terms of longterm trends in growth and stable isotope metrics at our study site. Our results suggest that increasing tree-ring iWUE at this site could partly be associated with leaf-level responses to increasing atmospheric CO₂ and stem morphological changes within Siberian Pine trees, as well as severe drought conditions during recent decades. Although the extent to which differences based on stem morphology might occur in other species or sites is unclear, the potential for diverging trends between stripbark and whole-bark trees across multiple tree-ring metrics should be considered and evaluated in future studies. An understanding of whether cambial dieback can impact longterm tree-ring trends will be critical for using these valuable, long-lived trees for paleoclimate reconstruction and for understanding the physiological behavior of ancient, strip-bark trees in general.

Acknowledgments

The authors would like to thank Khashaa Eldevochir and Jennie Zhu for their help with fieldwork, and Wei Huang from Lamont—Doherty Earth Observatory for her assistance with stable isotope measurements. We would also like to thank anonymous reviewers and all colleagues from the Lamont-Doherty Earth Observatory Tree-ring Laboratory for their feedback and suggestions.

Conflict of interest

None declared.

Funding

The Lamont-Doherty Earth Observatory Climate Center and the National Science Foundation (NSF award BCS-1210360 and OPP 17-37788) provided funding for this study. C.L. and N.D. were partially supported by the NSF Arctic Social Science Program project award number 2112463. D.M.B. was partially supported by AGL2015-73190-JIN and RYC-2017-23389 from the Spanish Ministry of Economy, Industry and Competitiveness.

Data availability

The tree-ring stable isotope data produced in this study can be found in the NCEI - NOAA paleoclimate data repository (https://www.ncei.noaa.gov/access/paleo-search/study/37239).

Authors' contributions

C.L. and L.A.H. designed and conducted the experiment; C.L. conducted statistical analyses and wrote the original draft of the manuscript; L.A.H., E.C., A.H. and N.P. were supervisors and involved in conceptual development; E.C., K.A., N.D. and D.M.B. assisted with data interpretation and provided feedback on methodology; O.B., B.N., N.P. and A.H. conducted fieldwork, assisted with project conceptualization and data collection and were involved in funding acquisition. All co-authors reviewed the manuscript and contributed edits.

References

Ababneh LN (2006) Analysis of radial growth patterns of strip-bark and whole-bark bristlecone pine trees in the White Mountains of California: implications in paleoclimatology and archaeology of the Great Basin. PhD Dissertation. The University of Arizona. The University of Arizona ProQuest Dissertations Publishing (3239535).

Andreu-Hayles L, Lévesque M, Guerrieri R, Siegwolf RTW, Körner C (2022) Limits and strengths of tree-ring stable isotopes. In: Siegwolf RTW, Brooks JR, Roden J, Saurer M (eds) Stable isotopes in tree rings: inferring physiological, climatic and environmental responses. Springer International Publishing, Cham, pp. 399–428. https://doi.org/10.1007/978-3-030-92698-4_14.

Andreu-Hayles L, Levesque M, Martin-Benito D, Huang W, Harris R, Oelkers R, Leland C, Martin-Fernández J, Anchukaitis KJ, Helle G (2019) A high yield cellulose extraction system for small whole wood samples and dual measurement of carbon and oxygen stable isotopes. Chem Geol 504:53–65.

Araguás-Araguás L, Froehlich K, Rozanski K (1998) Stable isotope composition of precipitation over southeast Asia. J Geophys Res Atmos 103:28721–28742.

Barbour MM (2007) Stable oxygen isotope composition of plant tissue: a review. Funct Plant Biol 34:83–94.

Belmecheri S, Lavergne A (2020) Compiled records of atmospheric CO₂ concentrations and stable carbon isotopes to reconstruct climate and derive plant ecophysiological indices from tree rings. Dendrochronologia 63:125748. https://doi.org/10.1016/j.de ndro.2020.125748.

Belmecheri S, Maxwell RS, Taylor AH, Davis KJ, Guerrieri R, Moore DJP, Rayback SA (2021) Precipitation alters the CO_2 effect on water-use efficiency of temperate forests. Glob Change Biol 27:1560–1571.

- Birks SJ, Edwards TWD (2009) Atmospheric circulation controls on precipitation isotope–climate relations in western Canada. Tellus B 61:566–576.
- Björklund J, Fonti MV, Fonti P, Van den Bulcke J, von Arx G (2021) Cell wall dimensions reign supreme: cell wall composition is irrelevant for the temperature signal of latewood density/blue intensity in Scots pine. Dendrochronologia 65:125785. https://doi.org/10.1016/j.de ndro.2020.125785.
- Boyce RL, Lubbers B (2011) Bark-stripping patterns in bristlecone pine (Pinus aristata) stands in Colorado, USA¹. J Torrey Botan Soc 138:308–321.
- Brienen RJW, Gloor E, Clerici S et al. (2017) Tree height strongly affects estimates of water-use efficiency responses to climate and CO₂ using isotopes. Nat Commun 8:288. http://www.nature.com/articles/s41467-017-00225-z (21 February 2019, date last accessed.
- Buchmann N, Kao W-Y, Ehleringer J (1997) Influence of stand structure on carbon-13 of vegetation, soils, and canopy air within deciduous and evergreen forests in Utah, United States. Oecologia 110:109–119.
- Bunn AG, Lawrence RL, Bellante GJ, Waggoner LA, Graumlich LJ (2003) Spatial variation in distribution and growth patterns of old growth strip-bark pines. Arctic, Antarctic, Alpine Res 35:323–330.
- Cabon A, Kannenberg SA, Arain A et al. (2022) Cross-biome synthesis of source versus sink limits to tree growth. Science 376:758–761.
- Campbell R, McCarroll D, Loader NJ, Grudd H, Robertson I, Jalkanen R (2007) Blue intensity in *Pinus sylvestris* tree-rings: developing a new palaeoclimate proxy. The Holocene 17:821–828.
- Cook ER, Krusic PJ (2014) ARSTAN. www.ldeo.columbia.edu/tree-ring-laboratory/resources/software. May 2018, date last accessed.
- Cook ER, Peters K (1997) Calculating unbiased tree-ring indices for the study of climatic and environmental change. The Holocene 7:361–370.
- D'Arrigo R, Jacoby G, Pederson N, Frank D, Buckley B, Nachin B, Mijiddorj R, Dugarjav C (2000) Mongolian tree-rings, temperature sensitivity and reconstructions of northern hemisphere temperature. The Holocene 10:669–672.
- Dansgaard W (1964) Stable isotopes in precipitation. Tellus 16:436–468.
- Davi NK, D'Arrigo R, Jacoby GC, Cook ER, Anchukaitis KJ, Nachin B, Rao MP, Leland C (2015) A long-term context (931–2005 C.E.) for rapid warming over Central Asia. Quat Sci Rev 121:89–97.
- Davi NK, Jacoby GC, Curtis AE, Baatarbileg N (2006) Extension of drought records for central Asia using tree rings: West-Central Mongolia*. J Climate 19:288–299.
- Davi NK, Rao MP, Wilson R et al. (2021) Accelerated recent warming and temperature variability over the past eight centuries in the central Asian Altai from blue intensity in tree rings. Geophys Res Lett 48. https://onlinelibrary.wiley.com/doi/10.1029/2021 GL092933. 16 February 2022, date last accessed.
- Duquesnay A, Bréda N, Stievenard M, Dupouey JL (1998) Changes of tree-ring δ 13C and water-use efficiency of beech (Fagus sylvatica L.) in north-eastern France during the past century. Plant, Cell & Environment 21:565–572.
- Farquhar GD, Ehleringer JR, Hubick KT (1989) Carbon isotope discrimination and photosynthesis. Annu Rev Plant Physiol Plant Mol Biol 40:503–537.
- Farquhar GD, Oleary MH, Berry JA (1982) On the relationship between carbon isotope discrimination and the intercellular carbon dioxide concentration in leaves. Funct Plant Biol 9:121–137.
- Field RD, Andreu-Hayles L, D'arrigo RD et al. (2021) Tree-ring cellulose $\delta 180$ records similar large-scale climate influences as precipitation $\delta 180$ in the northwest territories of Canada. Climate Dynam 58:759-776.

- Francey RJ, Farquhar GD (1982) An explanation of 13C/12C variations in tree rings. Nature 297:28–31.
- Frank DC, Poulter B, Saurer M et al. (2015) Water-use efficiency and transpiration across European forests during the anthropocene. Nat Clim Change 5:579–583.
- Fritts HC (1976) Tree rings and climate. Academic Press, London, UK. Gagen M, Battipaglia G, Daux V, Duffy J, Dorado-Liñán I, Hayles LA, Martínez-Sancho E, McCarroll D, Shestakova TA, Treydte K (2022) Climate signals in stable isotope tree-ring records. In: SIEGWOLF RTW, Brooks JR, Roden J, Saurer M (eds) Stable isotopes in tree rings. Springer International Publishing, Cham, pp. 537–579. https://link.springer.com/10.1007/978-3-030-92698-4_19. (12 October 2022, date last accessed).
- Gagen M, McCarroll D, Edouard J-L (2004) Latewood width, maximum density, and stable carbon isotope ratios of pine as climate indicators in a dry subalpine environment, French alps. Arctic, Antarctic, Alpine Res 36:166–171.
- Gagen M, McCarroll D, Loader NJ, Robertson I, Jalkanen R, Anchukaitis KJ (2007) Exorcising the 'segment length curse': summer temperature reconstruction since AD 1640 using non-detrended stable carbon isotope ratios from pine trees in northern Finland. The Holocene 17:435–446.
- Gessler A, Cailleret M, Joseph J, Schönbeck L, Schaub M, Lehmann M, Treydte K, Rigling A, Timofeeva G, Saurer M (2018) Drought induced tree mortality a tree-ring isotope based conceptual model to assess mechanisms and predispositions. New Phytol 219:485–490.
- Giguère-Croteau C, Boucher É, Bergeron Y, Girardin MP, Drobyshev I, Silva LCR, Hélie J-F, Garneau M (2019) North America's oldest boreal trees are more efficient water users due to increased [CO₂], but do not grow faster. Proc Natl Acad Sci 116:2749–2754.
- Graybill DA, Idso SB (1993) Detecting the aerial fertilization effect of atmospheric CO_2 enrichment in tree-ring chronologies. Global Biogeochem Cycles 7:81–95.
- Harris I, Jones PD, Osborn TJ, Lister DH (2014) Updated high-resolution grids of monthly climatic observations the CRU TS3.10 dataset: updated high-resolution grids of monthly climatic observations. Int J Climatol 34:623–642.
- Hessl AE, Anchukaitis KJ, Jelsema C, Cook B, Byambasuren O, Leland C, Nachin B, Pederson N, Tian H, Hayles LA (2018) Past and future drought in Mongolia. Sci Adv 4:e1701832. https://doi.org/10.1126/sciadv.1701832.
- Holmes RL (1983) Program COFECHA user's manual. Laboratory of Tree-Ring Research. The University of Arizona, Tucson.
- Huang R, Zhu H, Liu X, Liang E, Grießinger J, Wu G, Li X, Bräuning A (2017) Does increasing intrinsic water use efficiency (iWUE) stimulate tree growth at natural alpine timberline on the southeastern Tibetan Plateau? Global Planet Change 148:217–226.
- Jacoby GC, D'Arrigo RD, Davaajamts T (1996) Mongolian tree rings and 20th-century warming. Science 273:771–773.
- Kakinuma K, Yanagawa A, Sasaki T, Rao MP, Kanae S (2019) Socio-ecological interactions in a changing climate: a review of the Mongolian pastoral system. Sustainability 11:5883. https://doi.org/10.3390/su11215883.
- Kang S, Loader NJ, Wang J, Qin C, Liu J, Song M (2022) Tree-ring stable carbon isotope as a proxy for hydroclimate variations in semiarid regions of North-Central China. Forests 13:492. https://doi.org/10.3390/f13040492.
- Klesse S, Weigt R, Treydte K, Saurer M, Schmid L, Siegwolf RTW, Frank DC (2018) Oxygen isotopes in tree rings are less sensitive to changes in tree size and relative canopy position than carbon isotopes: oxygen isotopes in tree-rings are less sensitive. Plant Cell Environ. http://doi.wiley.com/10.1111/pce.13424. 26 September 2018, date last accessed.

- LaMarche VC (1969) Environment in relation to age of bristlecone pines. Ecology 50:53–59.
- Larson DW (2001) The paradox of great longevity in a short-lived tree species. Exp Gerontol 36:651–673.
- Larson DW, Matthes-Sears U, Kelly PE (1993) Cambial dieback and partial shoot mortality in Cliff-Face Thuja occidentalis: evidence for sectored radial architecture. Int J Plant Sci 154:496–505.
- Lavergne A, Graven H, De Kauwe MG, Keenan TF, Medlyn BE, Prentice IC (2019) Observed and modelled historical trends in the water-use efficiency of plants and ecosystems. Glob Change Biol 25:2242–2257.
- Leland C, Cook ER, Andreu-Hayles L et al. (2018) Strip-bark morphology and radial growth trends in ancient *Pinus sibirica* trees from Central Mongolia. J Geophys Res Biogeo 123:945–959.
- Liu X, An W, Leavitt SW, Wang W, Xu G, Zeng X, Qin D (2014) Recent strengthening of correlations between tree-ring δ^{13} C and δ^{18} O in Mesic western China: implications to climatic reconstruction and physiological responses. Global Planet Change 113:23–33.
- Liu X, Shao X, Liang E, Chen T, Qin D, An W, Xu G, Sun W, Wang Y (2009) Climatic significance of tree-ring δ^{18} O in the Qilian Mountains, northwestern China and its relationship to atmospheric circulation patterns. Chem Geol 268:147–154.
- Liu X, Zhao L, Voelker S et al. (2019) Warming and CO₂ enrichment modified the ecophysiological responses of Dahurian larch and Mongolia pine during the past century in the permafrost of northeastern China Cernusak L (ed). Tree Physiol 39:88–103.
- Liu Y, Wang L, Li Q, Cai Q, Song H, Sun C, Liu R, Mei R (2019) Asian summer monsoon-related relative humidity recorded by tree ring δ^{18} O during last 205 years. JGR Atmosph 124:9824–9838.
- Loader NJ, Helle G, Los SO, Lehmkuhl F, Schleser GH (2010) Twentieth-century summer temperature variability in the southern Altai Mountains: a carbon and oxygen isotope study of tree-rings. The Holocene 20:1149–1156.
- Loader NJ, Robertson I, Barker AC, Switsur VR, Waterhouse JS (1997) An improved technique for the batch processing of small wholewood samples to α -cellulose. Chem Geol 136:313–317.
- Loader NJ, Robertson I, McCarroll D (2003) Comparison of stable carbon isotope ratios in the whole wood, cellulose and lignin of oak tree-rings. Palaeogeogr, Palaeoclimatol, Palaeoecol 196:395–407.
- Marchand W, Girardin MP, Hartmann H, Depardieu C, Isabel N, Gauthier S, Boucher É, Bergeron Y (2020) Strong overestimation of water-use efficiency responses to rising CO₂ in tree-ring studies. Glob Chang Biol 26:4538–4558.
- Matthes U, Kelly PE, Ryan CE, Larson DW (2002) The formation and possible ecological function of stem strips in Thuja occidentalis. Int J Plant Sci 163:949–958.
- McCarroll D, Gagen MH, Loader NJ, Robertson I, Anchukaitis KJ, Los S, Young GHF, Jalkanen R, Kirchhefer A, Waterhouse JS (2009) Correction of tree ring stable carbon isotope chronologies for changes in the carbon dioxide content of the atmosphere. Geochim Cosmochim Acta 73:1539–1547.
- McCarroll D, Loader NJ (2004) Stable isotopes in tree rings. Quat Sci Rev 23:771–801.
- McCarroll D, Pettigrew E, Luckman A, Guibal F, Edouard J-L (2002) Blue reflectance provides a surrogate for latewood density of high-latitude pine tree rings. Arctic, Antarctic, Alpine Res 34:450–453.
- Pederson N, Hessl AE, Baatarbileg N, Anchukaitis KJ, Cosmo ND (2014) Pluvials, droughts, the Mongol Empire, and modern Mongolia. PNAS 111:4375–4379.
- Pederson N, Leland C, Nachin B, Hessl AE, Bell AR, Martin-Benito D, Saladyga T, Suran B, Brown PM, Davi NK (2013) Three centuries of shifting hydroclimatic regimes across the Mongolian breadbasket. Agric For Meteorol 178–179:10–20.

- Porter TJ, Pisaric MFJ, Field RD, Kokelj SV, Edwards TWD, deMontigny P, Healy R, LeGrande AN (2014) Spring-summer temperatures since AD 1780 reconstructed from stable oxygen isotope ratios in white spruce tree-rings from the Mackenzie Delta, northwestern Canada. Climate Dynam 42:771–785.
- Rao MP, Davi NK, D'Arrigo RD, Skees J, Nachin B, Leland C, Lyon B, Wang S-Y, Byambasuren O (2015) Dzuds, droughts, and livestock mortality in Mongolia. Environ Res Lett 10:074012. https://doi.org/10.1088/1748-9326/10/7/074012.
- Robertson A, Overpeck J, Rind D, Mosley-Thomps on E, Zielinski G, Lean J, Koch D, Penner J, Tegen I, Healy R (2001) Hypothesized climate forcing time series for the last 500 years. J Geophys Res 106:14783–14803.
- Roden J, Siegwolf R (2012) Is the dual-isotope conceptual model fully operational? Tree Physiol 32:1179–1182.
- Roden JS, Lin G, Ehleringer JR (2000) A mechanistic model for interpretation of hydrogen and oxygen isotope ratios in tree-ring cellulose. Geochim Cosmochim Acta 64:21–35.
- Rodriguez-Caton M, Andreu-Hayles L, Morales MS et al. (2021) Different climate sensitivity for radial growth, but uniform for tree-ring stable isotopes along an aridity gradient in *Polylepis tarapacana*, the world's highest elevation tree species Cernusak L (ed). Tree Physiol 41:1353–1371.
- Salzer MW, Hughes MK, Bunn AG, Kipfmueller KF (2009) Recent unprecedented tree-ring growth in bristlecone pine at the highest elevations and possible causes. Proc Natl Acad Sci 106:20348–20353.
- Sarris D, Siegwolf R, Körner C (2013) Inter- and intra-annual stable carbon and oxygen isotope signals in response to drought in Mediterranean pines. Agric For Meteorol 168:59–68.
- Sato T, Tsujimura M, Yamanaka T, Iwasaki H, Sugimoto A, Sugita M, Kimura F, Davaa G, Oyunbaatar D (2007) Water sources in semiarid Northeast Asia as revealed by field observations and isotope transport model. J Geophys Res 112:D17112. https://doi.org/10.1029/2006 JD008321.
- Saurer M, Aellen K, Siegwolf R (1997a) Correlating d13C and d180 in cellulose of trees. Plant, Cell Environ 20:1543–1550.
- Saurer M, Borella S, Schweingruber F, Siegwolf R (1997b) Stable carbon isotopes in tree rings of beech: climatic versus site-related influences. Trees 11:291–297.
- Saurer M, Schweingruber F, Vaganov EA, Shiyatov SG, Siegwolf R (2002) Spatial and temporal oxygen isotope trends at the northern tree-line in Eurasia. Geophys Res Lett 29:7-1–7-4.
- Saurer M, Siegwolf RTW, Schweingruber FH (2004) Carbon isotope discrimination indicates improving water-use efficiency of trees in northern Eurasia over the last 100 years. Glob Chang Biol 10:2109–2120.
- Saurer M, Spahni R, Frank DC et al. (2014) Spatial variability and temporal trends in water-use efficiency of European forests. Glob Chang Biol 20:3700–3712.
- Schauer AJ, Schoettle AW, Boyce RL (2001) Partial cambial mortality in high-elevation Pinus aristata (Pinaceae). Am J Bot 88:646–652.
- Scheidegger Y, Saurer M, Bahn M, Siegwolf R (2000) Linking stable oxygen and carbon isotopes with stomatal conductance and photosynthetic capacity: a conceptual model. Oecologia 125:350–357.
- Sidorova OV, Siegwolf RTW, Myglan VS, Ovchinnikov DV, Shishov VV, Helle G, Loader NJ, Saurer M (2013) The application of tree-rings and stable isotopes for reconstructions of climate conditions in the Russian Altai. Clim Change 120:153–167.
- Sidorova OV, Siegwolf RTW, Saurer M, Shashkin AV, Knorre AA, Prokushkin AS, Vaganov EA, Kirdyanov AV (2009) Do centennial tree-ring and stable isotope trends of Larix gmelinii (Rupr.) Rupr. Indicate increasing water shortage in the Siberian north? Oecologia 161:825–835.

- Stokes MA, Smiley TL (1968) An introduction to tree-ring dating. The University of Chicago Press, Chicago, USA.
- Szejner P, Wright WE, Babst F, Belmecheri S, Trouet V, Leavitt SW, Ehleringer JR, Monson RK (2016) Latitudinal gradients in tree ring stable carbon and oxygen isotopes reveal differential climate influences of the North American monsoon system: intraannual tree ring C and O isotopes. Eur J Vasc Endovasc Surg 121: 1978–1991.
- Tang K, Feng X, Funkhauser G (1999) The δ^{13} C of tree rings in full-bark and strip-bark bristlecone pine trees in the White Mountains of California. Glob Chang Biol 5:33–40.
- Vicente-Serrano SM, Beguería S, López-Moreno JI (2010) A multiscalar drought index sensitive to global warming: the standardized precipitation evapotranspiration index. J Climate 23:1696–1718.
- Voelker SL, Brooks JR, Meinzer FC et al. (2016) A dynamic leaf gas-exchange strategy is conserved in woody plants under changing ambient CO_2 : evidence from carbon isotope discrimination in paleo and CO_2 enrichment studies. Glob Change Biol 22: 889–902.
- Voltas J, Camarero JJ, Carulla D, Aguilera M, Ortiz A, Ferrio JP (2013) A retrospective, dual-isotope approach reveals individual predispositions to winter-drought induced tree dieback in the southernmost distribution limit of Scots pine: Scots pine disposition to winter-drought dieback. Plant Cell Environ 36:1435–1448.
- Vuille M, Werner M, Bradley RS, Keimig F (2005) Stable isotopes in precipitation in the Asian monsoon region. J Geophys Res 110: D23108.

- Wang L, Liu Y, Li Q, Song H, Cai Q, Sun C, Fang C, Liu R (2020a) A 210-year tree-ring δ^{18} O record in North China and its relationship with large-scale circulations. Tellus B 72:1770509. https://doi.org/10.1080/16000889.2020.1770509.
- Wang S, Zhang M, Che Y, Chen F, Qiang F (2016) Contribution of recycled moisture to precipitation in oases of arid Central Asia: a stable isotope approach: moisture recycling in oases of arid central Asia. Water Resour Res 52:3246–3257.
- Wang Y, Hu C, Ruan J, Johnson KR (2020) East Asian precipitation δ^{18} O relationship with various monsoon indices. J Geophys Res Atmos 125. https://onlinelibrary.wiley.com/doi/10.1029/2019 JD032282. 16 February 2022, date last accessed.
- Wigley TM, Briffa KR, Jones PD (1984) On the average value of correlated time series, with applications in dendroclimatology and hydrometeorology. J Appl Meteorol Climatol 23:201–213.
- Wright RD, Mooney HA (1965) Substrate-oriented distribution of bristlecone pine in the White Mountains of California. Am Midl Nat 73:257. https://doi.org/10.2307/2423454.
- Xu C, Zhao Q, An W, Wang S, Tan N, Sano M, Nakatsuka T, Borhara K, Guo Z (2021) Tree-ring oxygen isotope across monsoon Asia: common signal and local influence. Quat Sci Rev 269:107156. https://doi.org/10.1016/j.guascirev.2021.107156.
- Yamanaka T, Tsujimura M, Oyunbaatar D, Davaa G (2007) Isotopic variation of precipitation over eastern Mongolia and its implication for the atmospheric water cycle. J Hydrol 333:21–34.
- Zang C, Biondi F (2015) Treeclim: an R package for the numerical calibration of proxy-climate relationships. Ecography 38:431–436.